Dual Recognition and the Role of Specificity-Determining Residues in Colicin E9 DNase−Immunity Protein Interactions†

Wei Li,‡ Stefan J. Hamill,‡,§ Andrew M. Hemmings,‡,|| Geoffrey R. Moore,|| Richard James,‡ and Colin Kleanthous*,‡

Schools of Biological and Chemical Sciences, University of East Anglia, Norwich NR4 7TJ, U.K.

Received April 17, 1998; Revised Manuscript Received June 30, 1998

ABSTRACT: The immunity protein Im2 can bind and inhibit the noncognate endonuclease domain of the bacterial toxin colicin E9 with a K_d of 19 nM, 6 orders of magnitude weaker than that of the cognate immunity protein Im9 with which it shares 68% sequence identity. Previous work from our laboratory has shown that the specificity differences of these four-helix immunity proteins is due almost entirely to helix II which is largely variable in sequence in the immunity protein family. From alanine scanning mutagenesis of Im9 in conjunction with high-field NMR data, a dual recognition model for colicin−immunity protein specificity has been proposed whereby the conserved residues of helix III of the immunity protein act as the anchor of the endonuclease binding site while the variable residues of helix II control the specificity of the protein−protein interaction. In this work, we identify three residues (at positions 33, 34, and 38) in helix II which define the specificity differences of Im2 and Im9 for colicin E9 and, using alanine mutagenesis of the putative endonuclease binding surface of Im2, compare the distribution of binding energies for conserved and nonconserved sites in both immunity proteins. This comparison highlights the conserved residues of both Im2 and Im9 as the major determinants of E9 DNase binding energy. Conversely, the nonconserved, specificity-determining residues only contribute to the E9 DNase binding energy in the cognate Im9 protein, while in the noncognate immunity protein Im2, they either destabilize the complex or do not contribute to the binding energy. This comparative alanine scan of two immunity proteins therefore supports the dual recognition mechanism of selectivity in colicin−immunity protein interactions and provides a basis for understanding specificity in other protein−protein interaction systems involving structurally conserved protein families.

Specific macromolecular association involves the interplay of conserved and nonconserved structural elements which together define the specificity of the interaction. In protein−DNA recognition, for example, the conserved structure is the DNA duplex itself while the bases are the nonconserved element which offer the potential for sequence-specific interactions with protein. Unlike the major groove of DNA, the interfaces of protein−protein complexes are relatively flat undulating surfaces with little regular topology (*1*), making it difficult to ascertain how a protein might distinguish the appropriate binding partner from numerous alternatives which may be conserved in both sequence and structure. Such discrimination lies at the heart of signal transduction, hormone−receptor interactions, and the immune system, and it is this question of discrimination we have been addressing using bacterial toxin−inhibitor protein complexes from the colicin family of protein toxins.

Colicins are a diverse family of plasmid-encoded protein toxins synthesized by bacteria at times of nutrient or environmental stress as a means of reducing competition from other microbial populations (*2*, *3*). We have been studying the E group colicins which first bind the vitamin B_{12} transporter, BtuB, in combination with the porin OmpF (*4*, *5*) and then translocate across the outer membrane with the aid of the periplasmic proteins Tol Q, R, A, and B (*6*). Several cytotoxic activities have been ascribed to colicins, the most common being pore-forming ionophores that depolarize the cell by forming voltage-gated channels in the inner membrane (*7*). E colicins can also traverse the inner membrane and kill the cell through nuclease activity, targetted toward either 16S ribosomal RNA (ColE3; *8*, *9*) or the DNA of the bacterial chromosome (ColE2,[1] ColE7, ColE8, and ColE9; *10*−*13*). It is on this latter group that our work has been focused.

† This work was supported by The Wellcome Trust and by the Biotechnology & Biological Sciences Research Council. W.L. is supported by a UEA Research Based Studentship and an Overseas Research Students Award.

* Corresponding author: School of Biological Sciences, University of East Anglia, Norwich NR4 7TJ, U.K. Telephone: 44-1603-593221. Fax: 44-1603-592250. E-mail: c.kleanthous@uea.ac.uk.

‡ School of Biological Sciences.

§ Present address: Centre for Protein Engineering, MRC Centre, Hills Road, Cambridge CB2 2QH, U.K.

|| School of Chemical Sciences.

[1] Abbreviations: ColE9, colicin E9; ColE2, colicin E2; E9 DNase, isolated 15 kDa endonuclease domain of ColE9; Im2, immunity protein specific for ColE2; Im9, immunity protein specific for ColE9; k_{on}, association rate constant; k_{off}, dissociation rate constant; K_d, equilibrium dissociation constant.

S0006-2960(98)00862-9 CCC: $15.00
Published on Web 08/07/1998

Colicin-producing bacteria are immune to the action of their toxin because the cells also synthesize an immunity protein (~10 kDa) which binds to the cytotoxic domain and neutralizes its activity (*14*, *15*). In the case of the enzymatic colicins (~60 kDa), this complex is then released into the surrounding medium and it is as a complex that cell killing begins. An attractive feature of this system in terms of studying specificity in protein−protein interactions is that within the E group of colicins are four endonuclease-type toxins each requiring a specific immunity protein (Im2, Im7, Im8, and Im9). The 15 kDa endonuclease domains of the toxins (which can be overexpressed and purified separately; *16*) are ~65% identical in sequence, while the immunity protein family shares an overall sequence identity of ~50%. Since immunity proteins are inhibitors of both toxin and endonuclease activity, in vivo and in vitro assays of specificity are possible. Using such a combined approach, we have shown that immunity proteins exhibit both high affinity (*17*) and specificity (*18*) for their cognate colicins. The affinity of the colicin E9−Im9 complex, for example, is 0.1 fM in buffers with low ionic strengths, increasing to 18 fM in 200 mM salt. Nevertheless, other immunity proteins can provide protection for colicin E9 in biological plate assays, most often when overexpressed in bacterial cells, and the strength of this cross-reactivity is related directly to the in vitro binding affinity for that complex which can have values between nanomolar and millimolar (*18*). Therefore, the endonuclease colicins represent a unique system with which to address questions of specificity in protein−protein recognition since the affinities of these complexes span a range of almost 12 orders of magnitude.

Structural information in combination with protein engineering experiments is beginning to shed light on the molecular mechanism of immunity protein specificity. Diffracting crystals of the E9 DNase−Im9 complex have been obtained (*19*), and the crystal structure of Im7 and solution structure of Im9 have been published (*20*, *21*). Both immunity protein studies show the overall fold to be that of a distorted four-helix bundle (Figure 1), and subsequent high-field NMR data on Im9 binding to the 15 kDa E9 DNase identified helices II and III as the putative DNase binding surface (*22*). This was confirmed by alanine scanning mutagenesis across the two helices of Im9 which also quantitated their relative contribution to the binding energy (*23*). The highly conserved residues of helix III are the major determinants of complex stability, while the variable residues of helix II play a significant but lesser role. This was an intriguing observation since previous homologue scanning experiments had shown that helix II was almost entirely responsible for the colicin specificity of immunity proteins (*24*). We formulated a model based on these data to explain specificity in colicin−immunity protein interactions which we have called dual recognition (*23*, *25*). In this mechanism, the conserved elements of the colicin binding surface of an immunity protein act as the focus of the binding site while the variable specificity residues make both favorable and unfavorable interactions, the balance of which defines the specificity of the protein−protein interaction.

In this work, we set out to test the dual recognition model: first, by identifying individual residues in helix II which govern the specificity differences of Im2 and Im9 for the E9 DNase and, second, by investigating the contribution to the DNase binding energy of conserved and variable residues in the noncognate immunity protein Im2 and comparing these to those previously published for the cognate interaction of Im9. Our data fully support the dual recognition model and suggest that such a mechanism may underpin specificity in protein−protein recognition in other biological contexts.

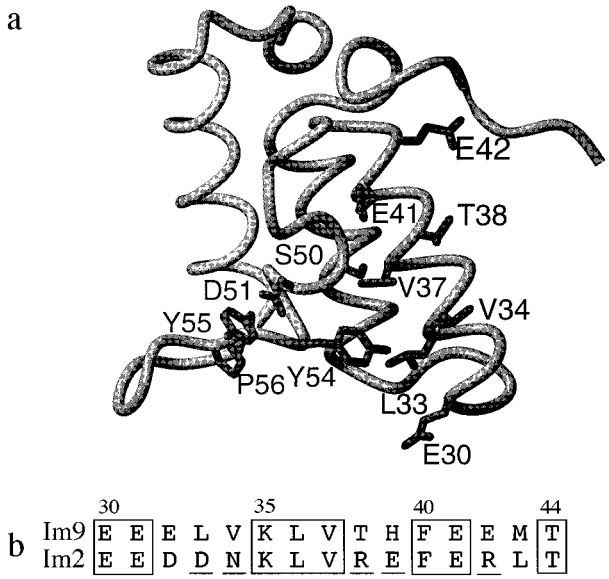

FIGURE 1: Residues targetted for mutagenesis. (a) The solution structure of Im9 (*21*) showing 12-residue side chains from helix II (residues 30−44) and helix III (residues 50−56), 10 of which form the main stabilizing interactions with the E9 DNase (*23*) as well as two other residues (Thr38 and Glu42) implicated in specificity. Although the structure of Im9 is shown, this study has focused on mutating these sites in the Im2 protein, for which a structure has yet to be determined but is likely to be very similar. Residues in helix III are identical between the two proteins. (b) Sequence alignment of helix II residues in Im9 and Im2. Potential specificity-determining residues (underlined) in Im2 were mutated to their corresponding counterparts in Im9.

MATERIALS AND METHODS

Materials, Bacterial Strains, and Plasmids. All chemicals and reagents were analytical grade, and were purchased from either Sigma or BDH. Restriction enzymes were purchased from Boehringer Mannheim. Colicin-sensitive *Escherichia coli* strain, JM83 *hsdR*, a restriction-deficient derivative of JM83 (*Ara+*, *Lac+*, *Pro*, *Thi*, *rpsL*, *ϕ80ΔlacZM15*), was used as the host strain. The expression vector pTrc99A was purchased from Pharmacia Biotech, and pCD01, with the *imm2* gene inserted between *Nco*I and *Hin*dIII sites of the vector, was used as the template for the site-directed mutagenesis.

PCR-Mediated Site-Directed Mutagenesis and Biological Plate Assays. Mutants were engineered as described by Li et al. (*24*). JM83 cells expressing wild-type and mutant immunity proteins were tested for ColE2 or ColE9 in vivo specificity using a biological plate assay as described previously (*24*). The concentrations of the ColE2 and ColE9 toxins were determined by Bradford assay.

Protein Purifications and Protein Determinations. Each mutant protein was purified from 1 L of JM83 cells containing the appropriate construct after induction for 6 h with 1 mM IPTG, as described previously for Im9 (*15*). Two

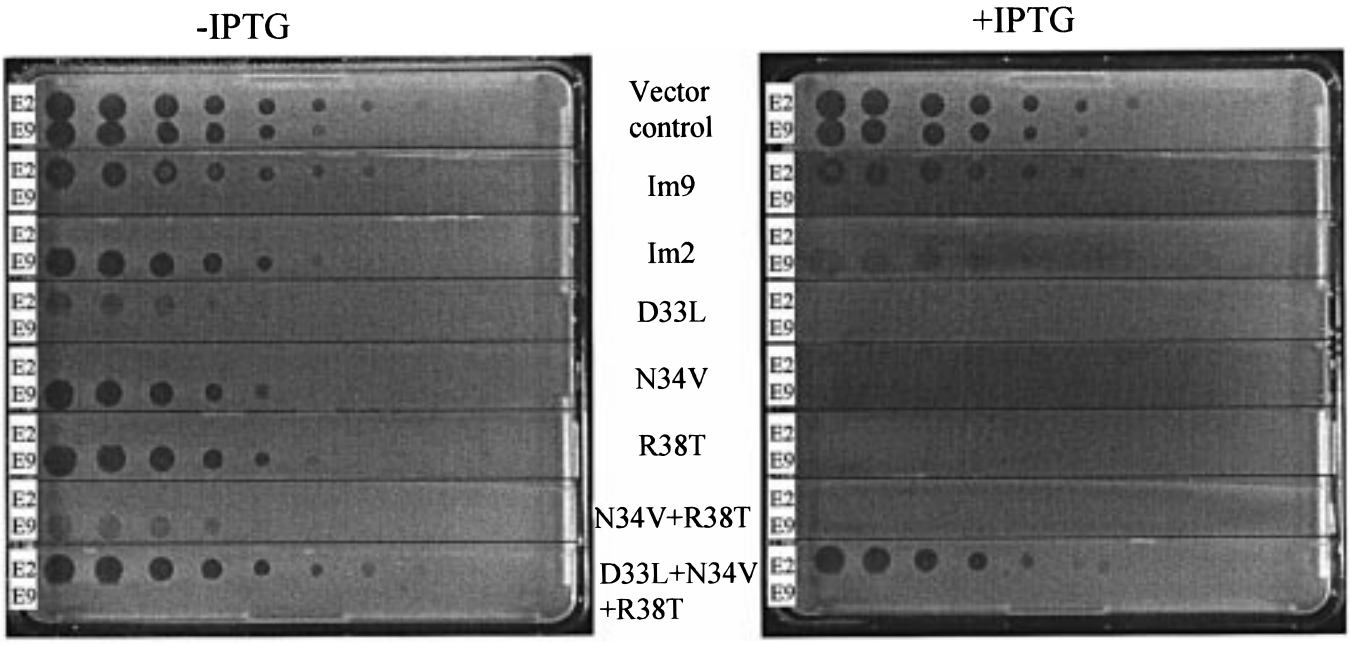

FIGURE 2: Biological phenotypes of Im2 specificity mutants. Agar plates (22 cm × 22 cm) were divided equally into eight lanes, and each lane was overlaid with *E. coli* JM83 cells haboring a different immunity protein construct or the vector. A serial 5-fold dilution from 3 mg/mL to 1.6 ng/mL, going from left to right, of either ColE2 (top of each lane) or ColE9 (bottom of each lane) was dropped onto each lawn of cells which had been grown either in the presence or in the absence of IPTG. The uppermost lane is the vector control and shows the cells to be sensitive to the action of both toxins. The absence of zones of killing indicates biological cross-reactivity with respect to the toxin by an immunity protein. The amino acid numbering corresponds to that in Figure 1 but refers to mutations in helix II of Im2 in which residues were substituted for those found in equivalent positions in Im9.

modifications were introduced. First, instead of using DNase and RNase treatment, sonication was used to break the cells to avoid DNase contamination. Second, after the final gel filtration column was used, the pooled fractions were dialyzed against dH_2O, lyophilized, and stored as a dried power at −20 °C. The E9 DNase was purified as described by Garinot-Schneider et al. (*26*). Protein concentrations were determined using a molar absorption coefficient of 17 550 M^{-1} cm^{-1} for E9 DNase and 11 400 M^{-1} cm^{-1} for Im9, Im2, and the Im2 mutant proteins.

Electrospray Ionization Mass Spectrometry. The masses of all mutant proteins were verified by electrospray mass spectrometry as described by Li et al. (*24*).

E9 DNase−Immunity Protein Dissociation Constants. The kinetic mechanism for complex formation between the E9 DNase and immunity proteins has recently been re-evaluated on the basis of high-field NMR data (*27*). The mechanism is shown in eq 1

$$N^* \overset{K_{eq}\sim 1}{\rightleftharpoons} N + I \overset{k_{on}}{\underset{k_{off}}{\rightleftharpoons}} NI \qquad (1)$$

where N is the nuclease and I is the immunity protein. The E9 DNase exists in two distinct conformations which interconvert slowly in solution and which are present at approximately equimolar amounts. Only one of these binds the immunity protein. The equilibrium K_d for complex formation can be calculated from the ratio of the individual dissociation (k_{off}) and association (k_{on}) rate constants, as has been previously reported by Wallis et al. (*17*, *18*). All experiments were conducted in 50 mM Mops buffer (pH 7.0) containing 200 mM NaCl and 1 mM dithiothreitol at 25 °C. Association of immunity proteins was monitored by stopped-flow fluorescence under pseudo-first-order conditions and the bimolecular rate constant obtained from linear replots of the rate of initial fluorescence enhancement versus the immunity protein concentration. Dissociation kinetics for E9 DNase−Im2 complexes were obtained either from radioactive subunit exchange (in which complexes were chased with [^{3}H]Im9) for slow dissociation rate constants ($<10^{-3}$ s^{-1}) or from fluorescence chase stopped flow (in which complexes were chased with an excess of Im9) for fast dissociation rate constants ($>10^{-3}$ s^{-1}).

Differences in binding energy for Im2 mutants and wild-type Im2 binding to the E9 DNase were determined according to eq 2

$$\Delta\Delta G_{binding} = RT \ln(K_d^{mutant}/K_d^{wild-type}) \qquad (2)$$

where R is the gas constant and T is the absolute temperature.

RESULTS

Identification of Immunity Protein Residues That Govern Colicin E9 Specificity. Previously, we identified helix II as the main determinant of colicin specificity in the immunity protein family by constructing a chimera in which helix II of Im9 was engineered into the Im2 framework. The resulting mutant exhibited complete Im9-like biological cross-reactivity when *E. coli* cells containing this construct were challenged with ColE9 (*24*). The purified chimeric protein was also analyzed for its ability to bind the E9 DNase domain in vitro, from which we found that the helix accounted for a 5 order of magnitude increase in binding affinity out of a total of 6 orders of magnitude difference between Im2 and Im9. Further chimeric constructs showed that the remaining 10-fold difference in binding affinity was due to internal packing interactions between helix II and helix I of the immunity protein.

Table 1: Kinetic and Thermodynamic Parameters for Im2 Specificity Mutants Binding the E9 DNase[a]

protein	k_{on} x 10^{-7} (M^{-1} s^{-1})[b]	k_{off} (s^{-1})[c]	K_d (M)[d]	$\Delta\Delta G$ (kcal/mol)[e]
Im2	5.0 (±0.3)	0.73 (±0.01)	1.5 (±0.1) × 10^{-8}	
Im9	10.6 (±0.3)	1.9 (±0.3) × 10^{-6}	1.8 (±0.3) × 10^{-14}	−8.1 (±0.1)
Im2 D33L	7.9 (±0.3)	3.8 (±0.1) × 10^{-3}	4.8 (±0.3) × 10^{-11}	−3.4 (±0.04)
Im2 N34V	5.1 (±0.8)	0.16 (±0.01)	3.3 (±0.7) × 10^{-9}	−0.9 (±0.1)
Im2 R38T	11.0 (±0.2)	0.29 (±0.05)	2.6 (±0.5) × 10^{-9}	−1.0 (±0.1)
Im2 E39H	5.6 (±0.3)	0.88 (±0.01)	1.6 (±0.1) × 10^{-8}	0.0 (±0.04)
Im2 R42E	6.3 (±0.2)	0.50 (±0.02)	8.0 (±0.6) × 10^{-9}	−0.4 (±0.1)
Im2 N34V/R38T	9.8 (±1.6)	1.8 (±0.1) × 10^{-2}	1.9 (±0.4) × 10^{-10}	−2.6 (±0.1)
Im2 D33L/N34V/R38T	11.5 (±0.8)	3.7 (±1.3) × 10^{-5}	3.4 (±1.4) × 10^{-13}	−6.4 (±0.3)
Im2 N34V/R38T/R42E	18.3 (±0.5)	1.2 (±0.1) × 10^{-2}	6.4 (±0.3) × 10^{-11}	−3.2 (±0.03)
Im2 N34V/R38T/E39H/R42E	14.5 (±2.0)	1.3 (±0.1) × 10^{-2}	9.5 (±1.5) × 10^{-11}	−3.0 (±0.1)

[a] All experiments were conducted in 50 mM Mops buffer (pH 7.0) containing 200 mM NaCl and 1 mM dithiothreitol at 25 °C. Standard errors from duplicate observations are shown in parentheses. [b] Immunity protein−E9 DNase association rate constants determined by stopped-flow fluorescence. [c] Immunity protein−E9 DNase dissociation rate constants determined by either radioactive or stopped-flow exchange kinetics. [d] Immunity protein−E9 DNase equilibrium dissociation constants calculated from the ratio of the dissociation and association rate constants. [e] $\Delta\Delta G$ calculated with respect to wild-type Im2 binding the E9 DNase domain.

Using site-directed mutagenesis in combination with biological plate assays of colicin immunity and kinetic and thermodynamic analyses, we set out in this work to identify the residues in helix II which are primarily responsible for the colicin specificity differences of Im2 and Im9. Helix II of Im9 contains 15 amino acids, eight of which are identical in Im2 and Im9 (Figure 1b). Of the seven remaining amino acid residues, two are similar (Glu and Asp, and Met and Leu) and five are different. Our mutagenesis experiments focused on the five variable residues, at positions 33, 34, 38, 39, and 42. A variety of single and multiple mutant constructs were engineered and their in vivo colicin cross-reactivities determined as described in Materials and Methods. A selection of biological plate assay results are presented in Figure 2. The ColE2 and ColE9 biological cross-reactivities of wild-type Im2- and Im9-containing *E. coli* cells were compared to those of a vector control and mutant proteins on the same agar plate under inducing (with IPTG) and noninducing (without IPTG) conditions. Earlier work in these systems (*18*, *24*) had shown that the two distinct induction regimes can detect a wide spectrum of biological cross-reactivities; in the absence of induction, only highly specific immunity proteins exhibit biological protection (due to "leakiness" in the repression of transcription in the vector system), whereas weak biological protection can be observed under inducing conditions where up to 40% of the cell protein is expressed immunity protein. As shown in Figure 2, the two parent immunity proteins Im2 and Im9 are both completely resistant to the action of their cognate toxin under both sets of conditions, since no zones of clearing (indicating cell death) are apparent, but are sensitive to the noncognate toxin in each case. As reported previously, Im2 shows partial cross-reactivity toward ColE9 under inducing conditions, a consequence of the nanomolar K_d exhibited by this protein for the E9 DNase (*18*).

Each of the five variable amino acids in helix II of Im2 was mutated singly to the amino acid found in Im9 and the mutant proteins assayed for biological activity toward ColE9 and ColE2. Only three mutants showed significant changes in specificity using this in vivo assay (Im2 D33L, Im2 N34V, and Im2 R38T) (Figure 2), while the remaining two mutants (Im2 E39H and Im2 R42E) displayed wild-type Im2 phenotypes (data not shown). Position 34 has already been identified by Wallis et al. (*28*) as a specificity determining residue, but in the context of Im9 to Im8 specificity. Im2 D33L had the most profound effect of all the mutants. This mutant behaved like Im9, displaying ColE9 but not ColE2 protection in the absence of IPTG, but unlike Im9 was still resistant to ColE2 when it was induced with IPTG. The mutations at positions 34 and 38 had less of an effect on specificity and displayed similar phenotypes; they were completely resistant to the action of both toxins when the bacterial cells were induced with IPTG but were essentially Im2-like in the absence of induction. When residues 34 and 38 were combined in a double mutant, however, they displayed significant biological cross-reactivity toward ColE9 in the absence of IPTG but were still resistant to the parent toxin, ColE2. It was only when all three mutants were combined (Im2 D33L/N34V/R38T) that the resulting immunity protein behaves exactly like Im9 on the biological plate assays under both inducing and noninducing conditions (Figure 2, bottom lane). Hence, the biological specificity differences of Im2 and Im9 for the ColE9 toxin are governed by just three residues of helix II, at positions 33, 34, and 38, with one (residue 33) playing the dominant role.

Kinetic Analysis of Im2 Specificity Mutants. Mutants were purified and characterized as reported previously (*24*) and summarized in Materials and Methods. The affinity of the mutant Im2 protein for the E9 DNase was obtained by determining the individual association and dissociation rate constants from which the equilibrium K_d could be calculated. Using this approach, K_ds ranging from 10^{-5} to 10^{-14} M can be obtained (*24*).

Immunity protein−E9 DNase association rate constants (k_{on}) were determined by stopped-flow fluorescence, as described previously (*17*, *18*, *23*, *24*). The association rate constant for Im9 under conditions of low ionic strength is essentially diffusion-controlled ($k_{on} = 4 \times 10^9$ M^{-1} s^{-1}) and shows a strong dependence on the salt concentration, decreasing to 9×10^7 M^{-1} s^{-1} in the presence of 200 mM salt, implying that electrostatic interactions play a major role in pre-aligning the immunity protein and the E9 DNase prior to collision (*17*). Consistent with this interpretation, the NMR structure of Im9 shows that the region of the protein predicted to make up the DNase binding site is negatively charged (*22*). Another important aspect of stopped-flow fluorescence-based, immunity protein−E9 DNase association measurements is the fact that they display biphasic kinetics.

An initial enhancement in the intrinsic tryptophan fluorescence, corresponding to the bimolecular collision, is followed by a first-order quench, thought to represent a conformational change in the DNase (*17*). Until recently, this conformational change was presumed to be after immunity binding; however, NMR data have now shown that free E9 DNase exists in two conformational states which interconvert slowly in solution (and are present at approximately equimolar amounts), and Im9 binds to one of these (*27*; see Materials and Methods). This more recent kinetic scheme is fully in accordance with the stopped-flow traces; indeed, the rate constant that is observed for the slow phase (4−5 s^{-1}) is similar to that calculated for the isomerization reaction by NMR.

Association kinetics for nine single and multiple site-directed mutants were determined by stopped-flow fluorescence in the presence of 200 mM salt. In every case, the first-order fluorescence quench, representing the isomerization in the E9 DNase, fell between 3 and 5 s^{-1} (data not shown). The bimolecular rate constants for these mutants are presented in Table 1 alongside both cognate (Im9) and noncognate (Im2) association rate constants, values for which were also obtained in this study and found to be very similar to those previously published (*18*, *24*). The association rate constant of Im9 is 2-fold faster than that of Im2, and it seems from the five single mutants at each of the variable positions in helix II that it is the loss of the positive charge at Arg38 which is primarily responsible for this difference (Table 1); the Im2 R38T mutant has essentially the same rate of association as Im9. Somewhat surprisingly, association rates greater than that seen for Im9 were obtained when both arginine mutations (R38T and R42E) were combined in Im2.

The dissociation rate constant (k_{off}) for immunity protein−E9 DNase complexes was obtained by one of two routes, depending on the magnitude of the rate constant. For slow dissociation rate constants ($<10^{-3}$ s^{-1}), a radioactive exchange experiment was employed (*17*), whereas for fast dissociation rate constants ($>10^{-3}$ s^{-1}), a stopped-flow exchange experiment was used (*18*). Stopped-flow-derived k_{off} data for three single and one double mutant are presented in Figure 3. Im2 dissociates from its complex with the E9 DNase with a rate constant of 0.73 s^{-1}, consistent with our previous estimate of 0.83 s^{-1} (*18*). k_{off} decreases for Im2 N34V and Im2 R38T by 4.5- and 2.5-fold, respectively, and this is readily observed from the slower stopped-flow displacement curves for these mutants in complex with the E9 DNase (Figure 3a). The double mutant of Im2 N34V/R38T, however, dissociates significantly slower than either mutant alone, showing a 40-fold reduction in k_{off} relative to that of Im2. Interestingly, when mutations at positions 39 and 42 are combined with this double mutant, there is no further decrease in k_{off} (Table 1), showing that these residues have little influence on DNase binding.

The value for the dissociation rate constant for the Im2 D33L mutant was sufficiently slow to be determined by radioactive exchange kinetics but fast enough to be estimated by stopped-flow kinetics. Since the two methods overlapped with this mutant and to eliminate the possibility of systematic error with any one technique, we used both to obtain k_{off}. k_{off} by stopped flow was $(3.8 \pm 0.1) \times 10^{-3}$ s^{-1} (inset of Figure 3b and Table 1), while k_{off} by radioactive exchange was $(6.0 \pm 2.3) \times 10^{-3}$ s^{-1} (data not shown), demonstrating

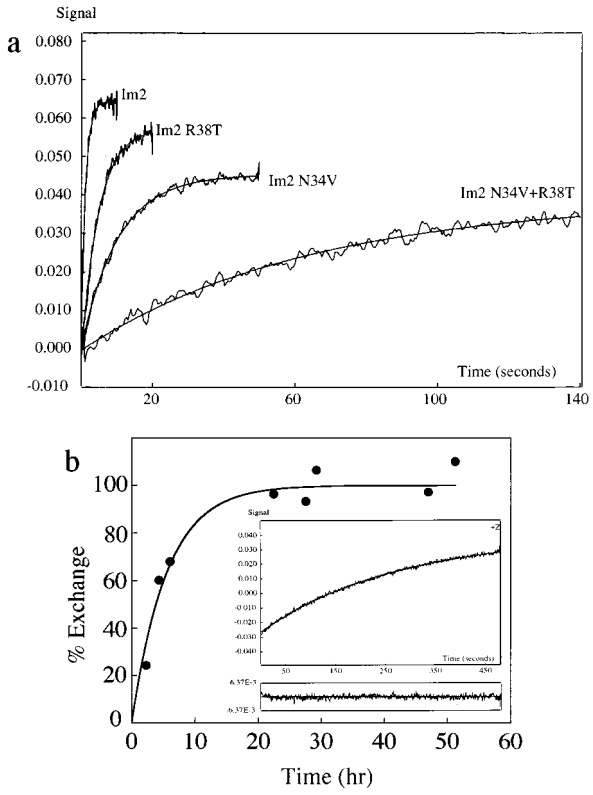

FIGURE 3: Dissociation rate constants for Im2 specificity mutants determined by exchange kinetics. (a) k_{off} determinations for Im2 specificity mutants at positions 34 and 38. Dissociation rate constants were obtained by stopped-flow tryptophan fluorescence. Conditions were as described in the footnote of Table 1 and Materials and Methods. The experiments are possible because the final fluorescence of the E9 DNase−Im2 complex is lower than that of the Im9 complex. Wild-type and mutant Im2 proteins in complex with the E9 DNase were chased with an excess of Im9 [see Wallis et al. (*18*) for further details] and the resulting traces fitted to a single-exponential rate equation, and these have been superimposed on the data. In each case, the residuals to the fits were random and below 5% of the overall change in fluorescence (data not shown). (b) k_{off} determinations for mutants incorporating position 33. The dissociation rate constant for Im2 D33L (inset) was determined as described above, and the residuals to the single-exponential fit are shown below the fluorescence trace. k_{off} for the triple mutant Im2 D33L/N34V/R38T was determined by radioactive exchange kinetics (main figure) as described in Materials and Methods and by Wallis et al. (*17*). The data are presented as the percentage of the total exchange and have been fitted to a single-exponential rate equation.

that there is reasonable agreement between the two methods and hence no systematic error. k_{off} for this single-site mutant is >190-fold slower than that for wild-type Im2. When this mutation is combined with the Im2 N34V and Im2 R38T mutations, k_{off} decreases by more than 4 orders of magnitude (Figure 3b) to 3.7×10^{-5} s^{-1}. The calculated equilibrium K_d values for the mutants (Table 1) indicate that the affinity of these protein−protein complexes is dominated by changes in the dissociation rate constant, consistent with previous work on colicin−immunity protein complexes (*18*, *23*). The most significant effect on K_d is seen in the Im2 D33L/N34V/R38T triple mutant which binds to the E9 DNase approximately 5 orders of magnitude tighter than wild-type Im2, close to that of Im9. Hence, three residues account for the major differences in affinity shown by Im2 and Im9 for the E9 DNase, and half of this is associated with a single mutation, Im2 D33L.

Table 2: Kinetic and Thermodynamic Parameters for Im2 Alanine Mutants Binding the E9 DNase[a]

protein	k_{on} x 10^{-7} (M^{-1} s^{-1})	k_{off} (s^{-1})	K_d (M)	$\Delta\Delta G$ (kcal/mol)
Im2	5.0 (±0.3)	0.73 (±0.01)	1.5 (±0.1) × 10^{-8}	
E30A	3.3 (±1.3)	7.1 (±1.6)	2.8 (±1.6) × 10^{-7}	1.6 (±0.4)
D33A	5.0 (±0.1)	0.61 (±0.06)	1.2 (±0.1) × 10^{-8}	−0.1 (±0.05)
N34A	8.9 (±0.1)	0.70 (±0.02)	7.9 (±0.3) × 10^{-9}	−0.4 (±0.02)
V37A	1.1 (±0.5)	81 (±1)	9.3 (±4.4) × 10^{-6}	3.7 (±0.3)
R38A	10.2 (±0.6)	0.24 (±0.02)	2.3 (±0.4) × 10^{-9}	−1.1 (±0.1)
E41A	0.4 (±0.01)	120 (±0)	3.0 (±0.1) × 10^{-5}	4.5 (±0.02)
R42A	6.0 (±1.2)	0.59 (±0.01)	1.0 (±0.2) × 10^{-8}	−0.3 (±0.1)
S50A	3.9 (±0.6)	34 (±2)	9.0 (±2.0) × 10^{-7}	2.4 (±0.1)
D51A	nd[b]	nd	≥10^{-4} [c]	≥5.8
Y54A	nd	nd	≥10^{-4}	≥5.8
Y55A	nd	nd	≥10^{-4}	≥5.8
P56A	1.3 (±0.2)	26 (±5)	2.1 (±0.7) × 10^{-6}	2.9 (±0.2)

[a] Experiments were conducted essentially as described in the legend of Figure 1 and in Materials and Methods. Standard errors from duplicate observations are shown in parentheses. [b] nd, not determined. [c] Alanine mutations at these positions significantly destabilize the colicin−immunity protein complex beyond that which we can measure using stopped-flow and exchange techniques ($K_d \sim 10^{-5}$ M). The K_d values for these mutants were estimated from biological plate assays in which the mutant Im2 proteins were challenged with ColE9 toxin. Unlike wild-type Im2, they fail to show any biological cross-reactivity, a situation reached by immunity proteins whose affinity for the colicin falls below ~10^{-4} M (*18*; K.-Y. Leung and W. Li, unpublished results).

Alanine Mutagenesis of E9 DNase Binding Residues in Im2. In our original alanine scan of Im9, more than 30 residues were mutated to alanine (*23*). Ten residues from helices II and III dominated E9 DNase binding and when mapped onto the surface of the unbound structure of Im9 were found to cluster together (Figure 1a), while the remaining residues, many of which either did not affect E9 DNase binding or only had small effects, flanked these important binding residues. The five conserved residues from helix III form a "hot spot" (*29*) accounting for about two-thirds of the binding energy. The other five residues from helix II lie next to this region and, while only contributing about one-third of the binding energy, define the specificity of the protein−protein interaction. Having identified the specificity-determining residues in Im2 and recognizing the importance of conserved residues in binding the E9 DNase, we mutated these residues in Im2 to alanine to test their importance to binding energy in a noncognate background.

The 10 residues from helices II and III were mutated singly to alanine along with Arg38 and Arg42 from helix II because they appear to play roles, albeit minor, in Im2 specificity. Thus, a total of 12 residues from Im2 were mutated to alanine (identified in Figure 1a), eight of which are conserved between Im2 and Im9 (including two residues in helix II) and four of which are variable residues. The mutants were overexpressed and the proteins purified, and their affinity for the E9 DNase was quantitated as described above. The K_d values for all 12 alanine mutants and the $\Delta\Delta G$ values for binding the E9 DNase are presented in Table 2. Binding could be detected for nine out of the 12 Im2 alanine mutants. Interestingly, the three Im2 mutants for which no E9 DNase binding was observed were those at conserved residues Asp51, Tyr54, and Tyr55, which contribute the bulk of the E9 DNase binding energy in the cognate immunity protein Im9 (*24*). These mutants could be produced in high yield and were not destabilized with respect to wild-type Im2 (data not shown). Even in biological plate assays, these mutants failed to show biological cross-reactivity against colicin E9, a situation which is reached when immunity proteins bind colicin toxins with a K_d of ≤10^{-4} M (*18*). Hence, a conservative estimate for the K_ds of these mutants is ~10^{-4} M.

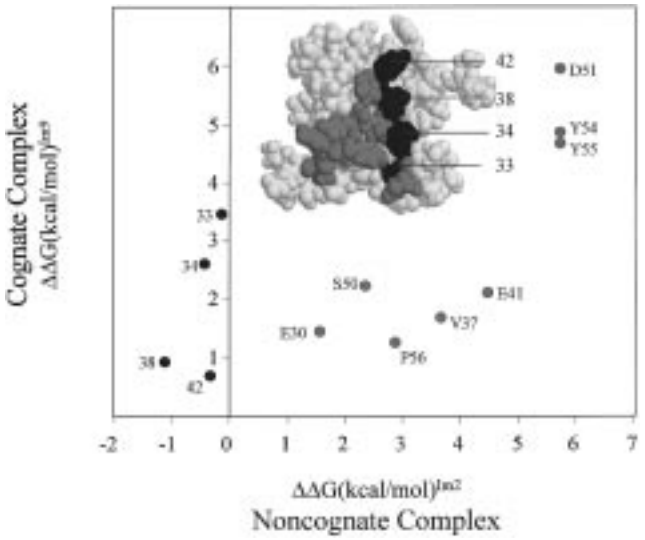

FIGURE 4: Comparative alanine scan of E9 DNase binding residues in Im2 and Im9. The figure shows $\Delta\Delta G_{binding}$ data for Im9 alanine mutants [taken from Wallis et al. (*23*)] plotted against $\Delta\Delta G_{binding}$ data for the equivalent alanine mutants in Im2 (data obtained in this study and listed in Table 2). Both sets of data were collected under identical conditions (see the footnote of Table 1). The inset shows a space-filling model of Im9 with residues colored according to the following scheme: red, mutated residues conserved in both proteins; blue, mutated residues not conserved; and yellow, residues not mutated. The data points on the graph are also colored according to this scheme. The identities of the blue residues in the two immunity proteins are as follows: Im9, Leu33, Val34, Thr38, and Glu42; and Im2, Asp33, Asn34, Arg38, and Arg42. Data points on the positive side of the *x*-axis identify mutations which perturb DNase binding in both proteins, while data points on the negative side of the *x*-axis identify mutations which only affect Im9 binding and either do not affect Im2 binding or enhance its binding to the E9 DNase.

To readily compare the effects on E9 DNase binding energy of substituting conserved and variable residues for alanine in both Im2 and Im9, $\Delta\Delta G$s for equivalent mutation sites in the two proteins are presented together in Figure 4. This is a particularly informative way to view the data since it compares the effects of mutating conserved residues in the two proteins (red in Figure 4) with the effects of mutating nonconserved residues (blue in Figure 4). It is evident that alanine mutants at conserved sites in both cognate (Im9) and noncognate (Im2) protein backgrounds lie on the positive side of the *x*-axis of the graph. Hence, in every case, these immunity protein mutations significantly affect E9 DNase binding (perturbing binding by 1−6 kcal/mol). In contrast, mutations at each of the variable (specificity-determining) residues lie on the negative side of the *x*-axis of the graph. This indicates that these residues either do not contribute to binding energy in the noncognate Im2 background or, as in the case of Im2 Arg38, act as a destabilizing interaction which when removed results in tighter binding of the E9 DNase.

DISCUSSION

Hierarchical Arrangement of Immunity Protein Specificity Determinants. Using both in vivo biological assays and in vitro binding affinities, we have demonstrated that the specificity differences of immunity proteins for a single colicin endonuclease are governed by only three residues at positions 33, 34, and 38 in helix II. Their contributions to specificity are not however equivalent. In both the in vivo (Figure 2) and in vitro (Figure 3 and Table 1) experiments, the relative importance of these residues is 33 > 34 ≈ 38. Substituting Asp33 of Im2 for leucine essentially switches the specificity of the protein from colicin E2 to colicin E9, the result of an increase in the binding affinity for the noncognate toxin of more than 250-fold. This mutant still however retains some ColE2 cross-reactivity but only when the cells are induced with IPTG, indicating that the affinity for its cognate toxin has decreased significantly (but this has yet to be analyzed in vitro). By contrast, the asparagine for valine and arginine for threonine substitutions at positions 34 and 38, respectively, only increase the affinity for the E9 DNase by 6- and 7-fold in each case, and these substitutions have small effects on biological cross-reactivity (Figure 2 and Table 1). The sum of the individual contributions of the three mutations to the E9 DNase binding energy is 5.3 kcal/mol, but when all three mutations are introduced into the same protein, the increase in the binding energy is 6.4 kcal/mol, which matches that obtained when the whole helix II from Im9 is inserted into the Im2 framework (*24*). Hence, these mutations show nonadditivity in binding energy (*30*), presumably because of their close proximity in helix II. While it is as yet unclear why position 33 is so important for specificity compared to the other residues in helix II, it seems reasonable to assume that it is due to its close association with the conserved residue Tyr54 which is critical for DNase binding. This highlights the interplay of conserved and nonconserved residues in defining specificity in this family of proteins. Furthermore, the fact that such dramatic specificity changes can be induced by a single substitution of a charged residue for a hydrophobic group also shows the importance of both types of interactions in protein−protein interaction specificity.

Comparison of the E9 DNase Binding Energetics of Im9 and Im2. Two important considerations stem from the dual recognition model. First, conserved residues are the major determinants of complex stability in all colicin−immunity protein complexes, and second, variable residues control specificity (and hence the final binding affinity) through a combination of favorable and unfavorable interactions. In the case of a cognate complex, where there are few unfavorable interactions, the maximal binding energy is obtained because the specificity sites dock into appropriate binding sites on the DNase. In noncognate complexes, however, while some binding energy is derived from conserved residues, specificity-determining residues do not contribute significantly to binding and might act as destabilizing entities within the complex, thus explaining the very much weaker affinities for these complexes.

The alanine scan of conserved and variable residues of the noncognate immunity protein Im2 provides strong support for the dual recognition model of protein−protein interaction specificity in this family of proteins. The conserved residues are clearly the focus of the binding interaction as they are with the cognate immunity protein Im9, and the relative importance of these interactions is also similar, although not identical (Table 2 and Figure 4). Importantly, however, the four specificity residues in Im2 do not contribute to the E9 DNase binding energy (particularly the critical specificity site, Asp33) and even destabilize the complex by ∼1.5 kcal/mol (N34A and R38A mutations). We can conclude therefore that the specificity differences between Im9 and Im2 for the E9 DNase involve the cooperation of conserved and variable residues, as predicted by the model. The conserved residues of Im2 provide the bulk of the binding energy, but this is insufficient to match the tight binding of Im9 because of two effects: (1) the additional binding energy that is achieved in the Im9 protein by having the appropriate residues at key specificity sites (predominantly residue 33 but including residues 34 and 38) and (2) the destabilization energy which comes from having inappropriate specificity residues in Im2 buried within the complex (particularly Arg38; Figure 4).

Dual Recognition and Specificity Mechanisms in Other Protein−Protein Interaction Systems. Specificity in protein−protein recognition has been investigated in a number of different biological contexts, such as antibody−antigen interactions (*31*), hematopoietic receptor complexes (*32*, and references therein), proteinase−inhibitor complexes (*33*), and RNase−inhibitor complexes (*34*). These studies revolved around crystal structures of the complexes coupled to a detailed breakdown of the energetics of the surfaces involved. It is of interest then to begin comparing such systems with colicin−immunity protein interactions.

Analysis of interprotein complexes (*1*, *35*) reveals that they involve large surfaces of each partner (generally encompassing >650 Å^2) becoming buried in the complex. Alanine scanning mutagenesis data on growth hormone binding to its receptor (*29*, *36*) and RNase inhibitor binding to RNase (*34*) have shown that even though up to 30 amino acid side chains of each protein may become buried at such interfaces only a fraction of these constitute energetically important interactions, and these tend to cluster together. However, this is not a universal phenomenon; for example, Dall'Acqua et al. (*37*) using an anti-hen egg white lysozyme antibody system have shown that in some cases the distribution of binding energies is not focused on a select few residues but rather is distributed throughout the binding epitope. Since the crystal structure of the E9 DNase−Im9 complex is not known, we cannot be certain of the extent of binding of the epitope on Im9, but the tightness of the complex (similar to that of the RNase−inhibitor systems) suggests that a significant amount of surface on Im9 will become buried in the complex. NMR amide perturbation analysis is consistent with this interpretation since it identified up to 26 residues in Im9 which might become buried on complex formation (*22*). The subsequent alanine scan of these and other residues indicated that only a fraction of those perturbed in the NMR experiments were energetically meaningful in complex stabilization (*23*). It seems likely then that this is an example of a complex for which the binding energetics are dominated by just a few residues.

Do these similarities between growth hormone binding to its receptor and RNase inhibitor binding to RNase with the

E9 DNase−Im9 complex extend to how specificity is encoded in these systems? Even with the present data, which only reflect one-half of the binding partnership, this seems unlikely to be the case. In each of the growth hormone and RNase systems, overlapping but nonidentical binding epitopes are employed to achieve specificity, with distinct hot spots of binding energy stabilizing a particular complex (*34*, *38*). Comparing the distribution of DNase binding energies for Im9 with Im2 (albeit on a limited number of residues) shows that they seem to have similar hot spots of binding energy since they are focused around the same conserved residues, but this is insufficient for tight binding (Figure 4). To achieve cognate binding ($K_d < 10^{-14}$ M), additional binding energy is needed which is supplied by the specificity-determining residues, primarily residues 33, 34, and 38 in helix II.

Dual recognition may be a common phenomenon in complexes involving structurally homologous proteins (*25*). T cell receptor interactions with self-peptide-bound major histocompatibility complex, for example, have been described as displaying "dual specificity" (*39*). This term was coined to emphasize the dual nature of the T cell receptor combining site which can recognize both the conserved helical jaws of the MHC molecule and the variable residues from the displayed peptide. The detailed energetics of these complexes have yet to be dissected, so it will be of interest to see whether they are comparable to those of colicin−immunity protein complexes. Other protein complexes which also seem to show dual recognition are signaling complexes involving SH2 and SH3 domains. These conserved domains recognize distinct peptide motifs, but specificity is mediated through neighboring variable residues (*40*).

In conclusion, dual recognition as a mechanism for defining protein−protein interaction specificity may be more widespread in biology than hitherto recognized. The basis for this mechanism is the close cooperation between conserved and variable residues at the interfacial regions of protein complexes, and this can result in a wide range of thermodynamic stabilities for the resulting complexes (*18*, *23*, *25*). As we have shown for colicin−immunity protein interactions, selectivity can be engendered through a few select residues which modulate the binding interactions from the conserved protein scaffold. In this way, the specificity of the protein−protein interaction can be fine-tuned without making significant changes to the character of the combining sites.

ACKNOWLEDGMENT

We thank Ann Reilly and Christine Moore for excellent technical assistance, the members of C. Kleanthous's lab for help and advice during the course of this work, Ruth Boetzel for Figure 1, and Russell Wallis for comments on the manuscript.

REFERENCES

1. Jones, S., and Thornton, J. M. (1996) *Proc. Natl. Acad. Sci. U.S.A. 93*, 13−20.
2. James, R., Lazdunski, C., and Pattus, F., Eds. (1992) *Bacteriocins, microcins and lantibiotics*, NATO ASI Series H, Springer, Heidelberg, Germany.
3. James, R., Kleanthous, C., and Moore, G. R. (1996) *Microbiology 142*, 1569−1580.
4. Di Masi, D. R., White, D. C., Schnaitman, C. A., and Bradbeer, C. (1973) *J. Bacteriol. 115*, 506−513.
5. Bénédetti, H., Frenette, M., Baty, D., Lloubès, R., Géli, V., and Lazdunski, C. (1989) *J. Gen. Microbiol. 135*, 3413−3420.
6. Webster, R. E. (1991) *Mol. Microbiol. 5*, 1005−1011.
7. Lazdunski, C. (1995) *Mol. Microbiol. 16*, 1059−1066.
8. Bowman, C. M., Dahlerg, J. E., Ikemura, T., Konisky, J., and Nomura, M. (1971) *Proc. Natl. Acad. Sci. U.S.A. 68*, 964−968.
9. Senior, B., and Holland, I. B. (1971) *Proc. Natl. Acad. Sci. U.S.A. 68*, 959−963.
10. Schaller, K., and Nomura, M. (1976) *Proc. Natl. Acad. Sci. U.S.A. 73*, 3989−3993.
11. Toba, M., Masaki, H., and Ohta, T. (1988) *J. Bacteriol. 170*, 3237−3242.
12. Eaton, T., and James, R. (1989) *Nucleic Acid Res. 17*, 1761−1761.
13. Chak, K.-F., Kuo, W.-S., Lu, F.-M., and James, R. (1991) *J. Gen. Microbiol. 137*, 91−100.
14. Jakes, K., and Zinder, N. D. (1974) *Proc. Natl. Acad. Sci. U.S.A. 71*, 3380−3384.
15. Wallis, R., Reilly, A., Rowe, A., Moore, G. R., James, R., and Kleanthous, C. (1992) *Eur. J. Biochem. 207*, 687−695.
16. Wallis, R., Reilly, A., Barnes, K., Abell, C., Campbell, D. G., Moore, G. R., James, R., and Kleanthous, C. (1994) *Eur. J. Biochem. 220*, 447−454.
17. Wallis, R., Moore, G. R., James, R., and Kleanthous, C. (1995) *Biochemistry 34*, 13743−13750.
18. Wallis, R., Leung, K.-Y., Pommer, A. J., Videler, H., Moore, G. R., James, R., and Kleanthous, C. (1995) *Biochemistry 34*, 13751−13759.
19. Kühlmann, U., Kleanthous, C., James, R., Moore, G. R., and Hemmings, A. M. (1998) *Acta Crystallogr., Sect. D* (in press).
20. Chak, K.-F., Safo, M. K., Ku, W.-Y., Hsieh, S.-Y., and Yuan, H. (1996) *Proc. Natl. Acad. Sci. U.S.A. 93*, 6437−6442.
21. Osborne, M. J., Breexe, A. L., Lian, L.-Y., Reilly, A., James, R., Kleanthous, C., and Moore, G. R. (1996) *Biochemistry 35*, 9505−9512.
22. Osborne, M. J., Wallis, R., Leung, K.-Y., William, G., Lian, L.-Y., James, R., Kleanthous, C., and Moore, G. R. (1997) *Biochem. J. 323*, 823−831.
23. Wallis, R., Leung, K.-Y., Osborne, M. J., James, R., Moore, G. R., and Kleanthous, C. (1998) *Biochemistry 37*, 476−485.
24. Li, W., Dennis, C. A., Moore, G. R., James, R., and Kleanthous, C. (1997) *J. Biol. Chem. 272*, 22253−22258.
25. Kleanthous, C., Hemmings, A. M., Moore, G. R., and James, R. (1998) *Mol. Microbiol. 28*, 227−233.
26. Garinot-Schneider, C., Pommer, A. J., Moore, G. R., Kleanthous, C., and James, R. (1996) *J. Mol. Biol. 260*, 731−742.
27. Whittaker, S. B.-M., Boetzel, R., MacDonald, C., Lian, L.-Y., Pommer, A. J., Reilly, A., James, R., Kleanthous, C., and Moore, G. R. (1998) *J. Biol. NMR* (in press).
28. Wallis, R., Moore, G. R., Kleanthous, C., and James, R. (1992) *Eur. J. Biochem. 210*, 923−930.
29. Clackson, T., and Wells, J. A. (1995) *Science 267*, 383−386.
30. Wells, J. A. (1990) *Biochemistry 29*, 8509−8517.
31. Davies, D. R., and Cohen, G. H. (1996) *Proc. Natl. Acad. Sci. U.S.A. 93*, 7−12.
32. Wells, J. A., and de Vos, A. M. (1996) *Annu. Rev. Biochem. 65*, 609−634.
33. Empie, M. W., and Laskowski, M. (1982) *Biochemistry 21*, 2274−2284.
34. Chen, C.-Z., and Shapiro, R. (1997) *Proc. Natl. Acad. Sci. U.S.A. 94*, 1761−1766.
35. Janin, J., and Chothia, C. (1990) *J. Biol. Chem. 265*, 16027−16030.
36. Cunningham, B. C., and Wells, J. A. (1993) *J. Mol. Biol. 234*, 554−563.

37. Dall'Aqua, W., Goldman, E. R., Eisenstein, E., and Mariuzza, R. A. (1996) *Biochemistry 35*, 9667−9676.
38. Cunningham, B. C., and Wells, J. A. (1991) *Proc. Natl. Acad. Sci. U.S.A. 88*, 3407−3411.
39. Garcia, K. C., Degano, M., Pease, L. R., Huang, M., Peterson, P. A., Teyton, L., and Wilson, I. A. (1998) *Science 279*, 1166−1172.
40. Pawson, T. (1995) *Nature 373*, 573−580.

BI9808621